AIAA JOURNAL
Vol. 30, No. 9, September 1992

Vibration of Spinning Ring-Stiffened Thin Cylindrical Shells

Shyh-Chin Huang* and Bih-Sheng Hsu†
National Taiwan Institute of Technology, Taipei, Taiwan 10772, Republic of China

The vibration characteristics (frequencies and mode shapes) of a spinning thin cylindrical shell with multiring stiffeners are investigated. The receptance theory is first derived for the spinning shell and spinning rings, in which the concept of "traveling harmonic line load" is introduced. The general frequency equation for a spinning ring-stiffened shell is derived. Numerical results for no spinning are compared with those of previous investigations, and precise agreement is obtained. For the spinning case, the results, obtained from the present approach, show that the ring stiffeners stiffen only the modes of higher circumferential wave number n. The effects of rotation on the reinforced shell and the phenomena of traveling mode shapes are also illustrated in detail in the paper.

Introduction

SPINNING shell elements have been widely used in mechanical, aeronautical, and marine engineering. The spinning of structures generates the Coriolis effects, and in consequence, the frequencies bifurcate and the modes become time dependent.[1,2] Ring elements are frequently used to stiffen the deflective response of shell. The vibration behavior of the shell-rings structures is, hence, of practical importance. Many researches have been devoted to the dynamic analysis of stationary cylindrical shell with ring stiffeners. Nevertheless, the analysis of spinning cylindrical shell-rings structures has not been seen in the literature. Because of Coriolis effects, the vibration behavior of the spinning shell-rings structure may differ significantly from the stationary one. The purpose of this research is to develop an analysis technique for joined spinning shell-rings structures and to investigate the effects of spinning on the structures' characteristics.

The major difficulty arising from the combination of shell and ring elements is the absence of exact shape functions. Wah and Hu[3] sketched the natural modes of the cylindrical shell reinforced with uniform, evenly spaced ring stiffeners. Garnet and Levy[4] investigated the same problem but treated the interaction between ring and shell as displacement-dependent forces. Al-Najafi and Warburton[5] employed the finite ring element to a similar problem, where partial experimental results were shown to verify their numerical results. Forsberg[6] cut a nonspinning shell-ring into shell and ring segments. Between segments, the compatibility and equilibrium conditions were enforced, and the concept of transfer matrix was applied to yield an overall system matrix. His derivation was, in a sense, exact; hence, his results provide a basis for validating our approach for the nonspinning case. Beskos and Oates[7] solved for the free and forced responses of ring-stiffened shells with the aid of dynamic stiffness influence coefficients. In fact, they employed the transfer matrix method in the paper. The receptance method, which was introduced by Bishop and Johnson,[8] was also developed to study the free vibration of the ring-stiffened shells by Wilken and Soedel[9,10] and of the reinforced plates by Kelkel.[11] The validity of the receptance method in evaluating the natural frequencies for such combined structures has been verified in their papers. Note that all of the papers just mentioned dealt with only nonspinning shells.

In this paper, the receptance approach is adopted for the analysis of a spinning ring-stiffened cylindrical shell. Unlike the traditional receptances, the authors introduce the concept of "traveling line receptance" in the paper so that the difficulty arising from the traveling modes is overcome. The frequency equation of the spinning shell with an arbitrary number of ring stiffeners (equal or unequal spacing) is then derived. Numerical results specialized for the stationary case ($\Omega = 0$) are first compared with those available in other investigations. Frequencies and mode shapes for up to four ring stiffeners are demonstrated. The effects of stiffeners and spinning speed on the frequencies of the reinforced shell are particularly discussed.

Mathematic Mode

A typical spinning cylindrical shell with a number of ring stiffeners is shown in Fig. 1. This research is intended to develop an approach to the vibration analysis of this combined structure. The receptance method[8] is extended and applied in this study. The major advantage of the receptance method is that it divides the system into subsystems and subsequently reduces the degree of complexity. The reinforced shell can be thought as a combination of two types of elements, the spinning shell and the spinning ring through certain line connections, as schematically shown in Fig. 2. Since the receptance method requires that the forced response of the elements due to loading on the connection lines be evaluated, the mathematic models and solution process for the spinning shell and the spinning ring are derived first.

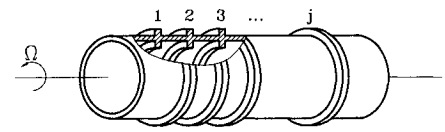

Fig. 1 Spinning cylindrical shell with multiring stiffeners.

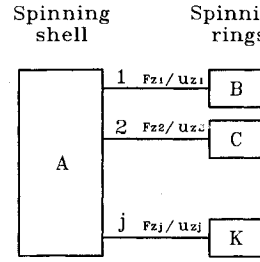

Fig. 2 Schematic diagram of the spinning shell with j spinning rings.

Received July 5, 1991; revision received Jan. 27, 1992; accepted for publication Jan. 29, 1992.

*Professor, Department of Mechanical Engineering, 43 Keelung Road, Section 4.
†Graduate Assistant.

Spinning Thin Shell

The equations of motion for a spinning cylindrical shell can be expressed as[12]

$$\{[L_L] + [L_R]\}\boldsymbol{u} = \boldsymbol{q} \tag{1}$$

where $[L_L]$ is the linear differential operator based on the Love-Timoshenko's theory for a nonspinning thin cylindrical shell,[13] and $[L_R]$ is a modifying operator resulting from rotation,[12] and $\boldsymbol{u} = \{u_x, u_\theta, u_z\}^T$ and $\boldsymbol{q} = \{-q_x, -q_\theta, q_z\}^T$ are the displacements vector and the pressure type loading vector, respectively.

The differential operators take the forms:

$$[L_L] = \begin{bmatrix} \left[\frac{K\partial^2}{l^2\partial\xi^2} + \frac{K(1-\nu)\partial^2}{2a^2\partial\theta^2} - \rho h\frac{\partial^2}{\partial t^2}\right] & \frac{K(1+\nu)}{2al}\frac{\partial^2}{\partial\xi\partial\theta} & \frac{\nu K}{al}\frac{\partial}{\partial\xi} \\ & \left[\frac{(1-\nu)}{2l^2}\left(K+\frac{D}{a^2}\right)\frac{\partial^2}{\partial\xi^2} + \left(\frac{D}{a^4}+\frac{K}{a^2}\right)\frac{\partial^2}{\partial\theta^2} - \rho h\frac{\partial^2}{\partial t^2}\right] & \left[-\frac{D}{a^4}\frac{\partial^3}{\partial\theta^3} + \frac{K}{a^2}\frac{\partial}{\partial\theta} - \frac{D}{a^2l^2}\frac{\partial^3}{\partial\xi^2\partial\theta}\right] \\ \text{sym.} & & \frac{D}{a^4}\nabla^4 + \frac{K}{a^2} + \rho h\frac{\partial^2}{\partial t^2} \end{bmatrix} \tag{2}$$

$$[L_R] = \begin{bmatrix} \rho h\Omega^2\frac{\partial^2}{\partial\theta^2} & 0 & 0 \\ & \rho h\Omega^2\frac{\partial^2}{\partial\theta^2} & 2\rho h\Omega^2\frac{\partial}{\partial\theta} - 2\rho h\Omega\frac{\partial}{\partial t} \\ \text{sym.} & & -\rho h\Omega^2\frac{\partial^2}{\partial\theta^2} \end{bmatrix} \tag{3}$$

where $\nabla^4 = \nabla^2\nabla^2$ is the biharmonic operator and $\nabla^2 = \partial^2/\partial\theta^2 + (a/l)^2\partial^2/\partial\xi^2$. $\xi = x/l$ and θ are the shell coordinates. $D = Eh^3/[12(1-\nu)]$ and $K = Eh/(1-\nu^2)$ represent the bending and membrane stiffnesses, respectively. ρ is the density, ν the Poisson's ratio, h the shell thickness, a the mean radius, and Ω the spinning speed. Note that $[L_L]$ and $[L_R]$ are symmetric based on the theory employed. The symmetry of differential operators ensures that the vibration frequencies of the shell are real,[13] and it is intuitively consistent with the physical system.

The simple supports are assumed on both ends, and the boundary conditions are

$$u_z(\xi, \theta, t) = 0$$
$$u_\theta(\xi, \theta, t) = 0 \qquad \text{at} \quad \xi = 0, 1 \tag{4a}$$

$$M_x(\xi, \theta\, t) = 0$$
$$N_x(\xi, \theta, t) = 0 \qquad \text{at} \quad \xi = 0, 1 \tag{4b}$$

where M_x and N_x, denoting the bending moment and membrane stress resultants, are of the expressions:

$$M_x = D\left[-\frac{1}{l^2}\frac{\partial^2 u_z}{\partial\xi^2} + \frac{\nu}{a^2}\left(\frac{\partial u_\theta}{\partial\theta} - \frac{\partial^2 u_z}{\partial\theta^2}\right)\right] \tag{4c}$$

$$N_x = K\left[\frac{1}{l}\frac{\partial u_x}{\partial\xi} + \frac{\nu}{a}\left(\frac{\partial u_\theta}{\partial\theta} + u_z\right)\right] \tag{4d}$$

A modal expansion technique for spinning shell has been developed by Huang and Soedel.[14] The forced response of the spinning shell after simplification is in terms of two generalized coordinates for each mn, where m denotes the longitudinal half wave number and n denotes the circumferential wave number:

$$\begin{aligned} u_x &= \sum_{m=1}^{\infty}\sum_{n=1}^{\infty} C_{mn}[\zeta_{mn}(t)\cos(n\theta) - \eta_{mn}(t)\sin(n\theta)]\cos(m\pi\xi) \\ u_\theta &= \sum_{m=1}^{\infty}\sum_{n=1}^{\infty} D_{mn}[\zeta_{mn}(t)\sin(n\theta) + \eta_{mn}(t)\cos(n\theta)]\sin(m\pi\xi) \\ u_z &= \sum_{m=1}^{\infty}\sum_{n=1}^{\infty} [\zeta_{mn}(t)\cos(n\theta) - \eta_{mn}(t)\sin(n\theta)]\sin(m\pi\xi) \end{aligned} \tag{5}$$

where C_{mn} and D_{mn} are the amplitude ratios of longitudinal and circumferential displacement to the radial displacement for each (m,n) mode.[15] ζ_{mn} and η_{mn} are two generalized coordinates. Substituting Eqs. (5) into Eq. (1) and using the orthogonality of trigonometric functions and the reduction process described in Ref. 15, one obtains the following differential equations:

$$\begin{Bmatrix}\ddot{\zeta}_{mn}\\ \ddot{\eta}_{mn}\end{Bmatrix} + \begin{pmatrix}0 & -\hat{\Omega}_{mn}\\ \hat{\Omega}_{mn} & 0\end{pmatrix}\begin{Bmatrix}\dot{\zeta}_{mn}\\ \dot{\eta}_{mn}\end{Bmatrix} + \begin{pmatrix}\hat{g}_{mn} & 0\\ 0 & \hat{g}_{mn}\end{pmatrix}\begin{Bmatrix}\zeta_{mn}\\ \eta_{mn}\end{Bmatrix} = \begin{Bmatrix}\hat{p}_{mn1}\\ \hat{p}_{mn2}\end{Bmatrix}, \qquad m, n = 1, 2, \ldots \tag{6}$$

where

$$\hat{\Omega}_{mn} = 2\Omega\frac{\begin{vmatrix}\hat{a} & -\hat{b} & 0\\ -\hat{b} & \hat{d} & 1\\ -\hat{c} & \hat{e} & D_{mn}\end{vmatrix}}{\Delta_{mn}} \tag{7a}$$

$$\hat{g}_{mn} = \frac{\begin{vmatrix}\hat{a} & -\hat{b} & -\hat{c}\\ -\hat{b} & \hat{d} & \hat{e}\\ -\hat{c} & \hat{e} & \hat{f}\end{vmatrix}}{\Delta_{mn}} \tag{7b}$$

$$\hat{p}_{mn1} = \frac{\begin{vmatrix}\hat{a} & -\hat{b} & Q_1\\ -\hat{b} & \hat{d} & Q_2\\ -\hat{c} & \hat{e} & Q_3\end{vmatrix}}{\Delta_{mn}} \tag{7c}$$

$$\hat{p}_{mn2} = \frac{\begin{vmatrix}\hat{a} & -\hat{b} & Q_4\\ -\hat{b} & \hat{d} & Q_5\\ -\hat{c} & \hat{e} & Q_6\end{vmatrix}}{\Delta_{mn}} \tag{7d}$$

$$\Delta_{mn} = \begin{vmatrix} \hat{a} & -\hat{b} & C_{mn} \\ -\hat{b} & \hat{d} & D_{mn} \\ -\hat{c} & \hat{e} & 1 \end{vmatrix} \tag{7e}$$

The shell parameters $\hat{a} \sim \hat{f}$ are listed in the Appendix and

$$\begin{Bmatrix} Q_1 \\ Q_2 \\ Q_3 \\ Q_4 \\ Q_5 \\ Q_6 \end{Bmatrix} = \frac{2}{\rho h \pi} \int_0^1 \int_0^{2\pi} \begin{Bmatrix} q_x \cos(m\pi\xi) \cos(n\theta) \\ q_\theta \sin(m\pi\xi) \sin(n\theta) \\ q_z \sin(m\pi\xi) \cos(n\theta) \\ -q_x \cos(m\pi\xi) \sin(n\theta) \\ q_\theta \sin(m\pi\xi) \cos(n\theta) \\ -q_z \sin(m\pi\xi) \sin(n\theta) \end{Bmatrix} d\theta \, d\xi \tag{8}$$

Note that, in Eq. (8), the various q are functions of time and space. Equation (6) is a discretized equation and has been proven[12] to be an accurate model containing both in- and extensional modes.

The receptance method requires a harmonic input acting on the connecting line in order to formulate the frequency equation of the combined system. Because the modes of a spinning shell are time dependent (traveling),[15] this paper introduces the concept of traveling harmonic line load acting on the shell, i.e., $q_x = q_\theta = 0$, and

$$q_z = \frac{F_z}{l} \delta(\xi - \xi^*) e^{i(s\theta + \omega t)}, \qquad s = 1, 2, 3, \ldots \tag{9}$$

where F_z is the force magnitude in the transverse direction, ξ^* the axial location of load (ring location), ω the driving frequency, and s the specified (input) circumferential wave number in load. Note that in Eq. (9), unlike the traditional line receptance, the line force has the space variable θ coupled with the time. Figure 3 illustrates the shell coordinates and the traveling line load of $s = 3$. Substituting Eq. (9) into Eq. (8), it is obtained that $Q_1 = Q_2 = Q_4 = Q_5 = 0$ and

$$Q_3 = \frac{2F_z}{\rho h l} \sin(m\pi\xi^*) e^{i\omega t}, \qquad s = n \tag{10a}$$

$$= 0, \qquad s \neq n \tag{10b}$$

$$Q_6 = \frac{2F_z}{\rho h l} \sin(m\pi\xi^*) i e^{i\omega t}, \qquad n = n \tag{10c}$$

$$= 0, \qquad s \neq n \tag{10d}$$

Thus, from Eqs. (7c) and (7d), one obtains that the generalized forces for each mn are

$$\begin{Bmatrix} \hat{p}_{mn1} \\ \hat{p}_{mn2} \end{Bmatrix} = \frac{2F_z}{\rho h l} \frac{(\hat{a}\hat{d} - \hat{b}^2)}{\Delta_{mn}} \sin(m\pi\xi^*) \begin{Bmatrix} 1 \\ -i \end{Bmatrix} e^{i\omega t} \tag{11}$$

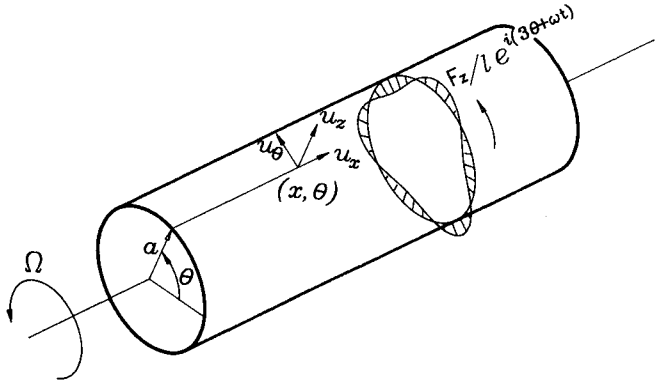

Fig. 3 Coordinates for the spinning shell and the harmonic traveling line load.

Subsequently, Eq. (6) yields that

$$\begin{Bmatrix} \zeta_{mn} \\ \eta_{mn} \end{Bmatrix} = \frac{2F_z}{\rho h l} \frac{(\hat{a}\hat{d} - \hat{b}^2)}{\Delta_{mn}} \times \frac{e^{i\omega t}}{(-\omega^2 + \hat{g}_{mn}) - \hat{\Omega}_{mn}\omega} \sin(m\pi\xi^*) \begin{Bmatrix} 1 \\ -i \end{Bmatrix} \tag{12}$$

$$m = 1, 2, 3, \ldots \qquad n = s$$

The steady-state response of the transverse displacement u_z is then solved to be

$$u_z(\xi, \theta, t) = \frac{2F_z}{\rho h l} \sum_{m=1}^{\infty} \frac{(\hat{a}\hat{d} - \hat{b}^2)}{\Delta_{mn}} \times \frac{e^{i(n\theta + \omega t)}}{(-\omega^2 + \hat{g}_{mn}) - \hat{\Omega}_{mn}\omega} \sin(m\pi\xi^*) \sin(m\pi\xi) \tag{13}$$

It is noticed that the natural frequencies (ω_{mn}) of the spinning shell can also be solved from Eq. (6), and after arrangement, they are of the values:

$$\omega_{mn_{1,2}} = -\tfrac{1}{2}\left(\hat{\Omega}_{mn} \mp \sqrt{\hat{\Omega}_{mn}^2 + 4\hat{g}_{mn}}\right) \tag{14}$$

The denominator of Eq. (13) is, hence, rewritten in terms of the spinning shell frequencies, $\omega_{mn_{1,2}}$ and the harmonic driving frequency ω as

$$u_z(\xi, \theta, t) = -\frac{2F_z}{\rho h l} \sum_{m=1}^{\infty} \frac{(\hat{a}\hat{d} - \hat{b}^2)}{\Delta_{mn}} \times \frac{e^{i(n\theta + \omega t)}}{(\omega - \omega_{mn1})(\omega - \omega_{mn2})} \sin(m\pi\xi^*) \sin(m\pi\xi) \tag{15}$$

where $n = 1, 2, 3, \ldots$.

Spinning Thin Ring

The equations of motion of a spinning ring are expressed as[16]

$$L_z(u_z, u_\theta) + \rho h \ddot{u}_z - 2\rho h \Omega \dot{u}_\theta = q_z \tag{16a}$$

$$L_\theta(u_z, u_\theta) + \rho h \ddot{u}_\theta - 2\rho h \Omega \dot{u}_z = q_\theta \tag{16b}$$

where u_z and u_θ are the deflections of the ring in radial and tangential directions, respectively, q_z and q_θ are the distributed loads, and L_z and L_θ are differential operators:

$$L_z(u_z, u_\theta) = \frac{D}{a^4}(u_z''' - u_\theta'') + \frac{K}{a^2}(u_z + u_\theta') - \rho h \Omega^2 (u_z'' - 2u_\theta') \tag{17a}$$

$$L_\theta(u_z, u_\theta) = \frac{D}{a^4}(u_z''' - u_\theta'') - \frac{K}{a^2}(u_z' + u_\theta'') - \rho h \Omega^2 (2u_z' - u_\theta'') \tag{17b}$$

in which the primes denote the differentiations with respect to θ; D and K represent the bending and membrane stiffnesses of the ring, respectively; ρ is the density, ν the Poisson's ratio, h the ring thickness, and a the mean radius.

Because of the periodic nature of the displacement functions u_z and u_θ in θ, and with the inextensional assumption, i.e., $u_z = -u_\theta'$, it is appropriate to assume the displacement functions to be[16]

$$u_z(\theta, t) = \sum_{n=1}^{\infty} [\epsilon_n(t) \cos(n\theta) + \vartheta_n(t) \sin(n\theta)] \tag{18a}$$

$$u_\theta(\theta, t) = \sum_{n=1}^{\infty} [(1/n)\vartheta_n(t) \cos(n\theta) - (1/n)\epsilon_n(t) \sin(n\theta)] \tag{18b}$$

where ϵ_n and ϑ_n are two generalized coordinates. By similar procedures as done for shell, ϵ_n and ϑ_n can be solved from the

following differential equations

$$\begin{Bmatrix} \ddot{\epsilon}_n \\ \ddot{\vartheta}_n \end{Bmatrix} + \begin{pmatrix} 0 & -\bar{\Omega}_n \\ \bar{\Omega}_n & 0 \end{pmatrix} \begin{Bmatrix} \dot{\epsilon}_n \\ \dot{\vartheta}_n \end{Bmatrix} + \begin{pmatrix} \bar{g}_n & 0 \\ 0 & \bar{g}_n \end{pmatrix} \begin{Bmatrix} \epsilon_n \\ \vartheta_n \end{Bmatrix} = \begin{Bmatrix} \bar{p}_{n1} \\ \bar{p}_{n2} \end{Bmatrix} \quad (19)$$

where

$$\bar{\Omega}_n = 2\Omega \frac{(\bar{b} + n\bar{a})}{(\bar{a} + n\bar{b})} \quad (20a)$$

$$\bar{g}_n = \frac{n(\overline{bc} - \bar{a}^2)}{(\bar{a} + n\bar{b})} \quad (20b)$$

$$\bar{p}_{n1} = \frac{n(Q_1\bar{b} - \bar{a}Q_4)}{(\bar{a} + n\bar{b})} \quad (20c)$$

$$\bar{p}_{n2} = \frac{n(Q_2\bar{b} - \bar{a}Q_3)}{(\bar{a} + n\bar{b})} \quad (20d)$$

The parameters $\bar{a} \sim \bar{c}$ are listed in the Appendix and

$$\begin{Bmatrix} Q_1 \\ Q_2 \\ Q_3 \\ Q_4 \end{Bmatrix} = \frac{1}{\rho h \pi} \int_0^{2\pi} \begin{Bmatrix} q_z \cos(n\theta) \\ q_z \sin(n\theta) \\ q_\theta \cos(n\theta) \\ q_\theta \sin(n\theta) \end{Bmatrix} d\theta \quad (20e)$$

Note also that q_z and q_θ are functions of θ and t. As previously, a traveling harmonic line load in transverse direction is assumed, i.e., $q_\theta = 0$, and

$$q_z = (F_z/b)e^{i(s\theta + \omega t)}, \qquad s = 1, 2, 3, \ldots \quad (21)$$

where b is the width of the ring. It is obtained that $Q_3 = Q_4 = 0$ and

$$Q_1 = \frac{F_z}{\rho h b} e^{i\omega t}, \qquad s = n \quad (22a)$$

$$= 0, \qquad s \neq n \quad (22b)$$

$$Q_2 = \frac{iF_z}{\rho h b} e^{i\omega t}, \qquad s = n \quad (22c)$$

$$= 0, \qquad s \neq n \quad (22d)$$

From Eqs. (20c) and (20d), the forcing terms in Eq. (19) for each mn are evaluated to be

$$\begin{Bmatrix} \bar{p}_{n1} \\ \bar{p}_{n2} \end{Bmatrix} = \frac{F_z}{\rho h b} \frac{n\bar{b}}{\bar{a} + n\bar{b}} \begin{Bmatrix} 1 \\ i \end{Bmatrix} e^{i\omega t} \quad (23)$$

Subsequently,

$$\begin{Bmatrix} \epsilon_n \\ \vartheta_n \end{Bmatrix} = \frac{F_z}{\rho h b} \frac{n\bar{b}}{\bar{a} + n\bar{b}} \frac{e^{i\omega t}}{(-\omega^2 + \bar{g}_n) + \bar{\Omega}_n \omega} \begin{Bmatrix} 1 \\ i \end{Bmatrix} \quad (24)$$

The steady-state response of the spinning ring is then obtained from Eqs. (16) as

$$u_z(\theta\, t) = \frac{F_z}{\rho h b} \frac{n\bar{b}}{\bar{a} + n\bar{b}} \frac{e^{i(n\theta + \omega t)}}{(-\omega^2 + \bar{g}_n) + \bar{\Omega}_n \omega}, \qquad n = 1, 2, 3, \ldots \quad (25a)$$

In the same manner, the denominator of Eq. (25a) can be rewritten in terms of the spinning ring frequencies, $\omega_{n_{1,2}}$, and the harmonic driving frequency ω as

$$u_z(\theta\, t) = -\frac{F_z}{\rho h b} \frac{n\bar{b}}{\bar{a} + n\bar{b}} \frac{e^{i(n\theta + \omega t)}}{(\omega - \omega_{n_1})(\omega - \omega_{n_2})}, \qquad n = 1, 2, 3, \ldots \quad (25b)$$

Frequency Equation of the Spinning Ring-Stiffened Shell

The receptance method is to be applied to join the spinning shell and the spinning rings to yield the frequency equation. A receptance is defined as the ratio of a steady-state deflection response at a certain point to a harmonic force or moment input at the same or at a different point,[8] i.e.,

$$\alpha_{ij} = \frac{\text{deflection response of system } A \text{ at location } i}{\text{harmonic force or moment input of system } A \text{ at location } j} \quad (26)$$

where α_{ii} is called the direct receptance and α_{ij} $(i \neq j)$ is the cross receptance. For a shell with ring attachment, each circular line where the ring is attached can be thought as a connecting point. Hence, the structure can be treated as a shell connected to j rings by one junction to each of them, as shown in Fig. 2. Each connection represents a circular line of radial displacement constraint. Note that in reality there should be a three-way constraint, radial, tangential, and axial for each ring attachment. The tangential constraint is, however, implied already though the radial displacement constraint in the derivation of Eqs. (6) and (19).[12] The axial constraint between shell and ring is ignored in the same manner as described in Ref. 4. It will be seen, from the comparison with other studies, that with the present shell theory as simple as a radial constraint for each ring and shell, it is enough for lower modes. The frequency equation for the joined system is[8]

$$\begin{vmatrix} \alpha_{11} + \beta_1 & \alpha_{12} & \alpha_{13} & \cdots & \alpha_{1j} \\ \alpha_{21} & \alpha_{22} + \beta_2 & \alpha_{23} & \cdots & \alpha_{2j} \\ \alpha_{31} & \alpha_{12} & \alpha_{33} + \beta_3 & \cdots & \alpha_{3j} \\ \vdots & \vdots & \vdots & & \vdots \\ \alpha_{j1} & \alpha_{j2} & \alpha_{j3} & \cdots & \alpha_{jj} + \beta_j \end{vmatrix} = 0 \quad (27)$$

where α denote the receptances of the spinning shell, and β_1, $\beta_2, \ldots, \beta_j$ are the receptances of the spinning rings. From Eq. (15), the receptances of the spinning shell are obtained as

$$\alpha_{ij} = -\frac{2}{\rho_s h_s l} \sum_{m=1}^{\infty} \frac{(\hat{a}\hat{d} - \hat{b}^2)}{\Delta_{mn}} \frac{\sin(m\pi\xi_i)\sin(m\pi\xi_j)}{(\omega - \omega_{mn1})(\omega - \omega_{mn2})}, \qquad n = 1, 2, 3, \ldots \quad (28)$$

Assuming all of the rings are the same, Eqs. (25) and (26) yield

$$\beta_1 = \beta_2 = \cdots = \beta_j = -\frac{1}{\rho_r h_r b} \frac{n\bar{b}}{\bar{a} + n\bar{b}} \frac{1}{(\omega - \omega_{n1})(\omega - \omega_{n2})}, \qquad n = 1, 2, 3, \ldots \quad (29)$$

Note that subscripts s and r are added in Eqs. (28) and (29) to distinguish the parameters between shell and ring.

First of all, the simplest case of one ring stiffener (attached at ξ_1) is discussed. For this case, the frequency equation becomes

$$\alpha_{11}(\omega) + \beta_1(\omega) = 0 \quad (30a)$$

or in detail

$$\frac{2}{\rho_s h_s l} \sum_{m=1}^{\infty} \left[\frac{(\hat{a}\hat{d} - \hat{b}^2)}{\Delta_{mn}} \frac{\sin^2(m\pi\xi_1)}{(\omega - \omega_{mn1})(\omega - \omega_{mn2})} \right] + \frac{1}{\rho_r h_r b} \frac{n\bar{b}}{\bar{a} + n\bar{b}} \times \frac{1}{(\omega - \omega_{n1})(\omega - \omega_{n2})} = 0, \qquad n = 1, 2, 3, \ldots \quad (30b)$$

Equation (30b), when $\Omega = 0$, yields the same expression as that in Ref. 9. For the spinning ring-stiffened shell, Eq. (30b), however, is the only equation available for frequency calculation.

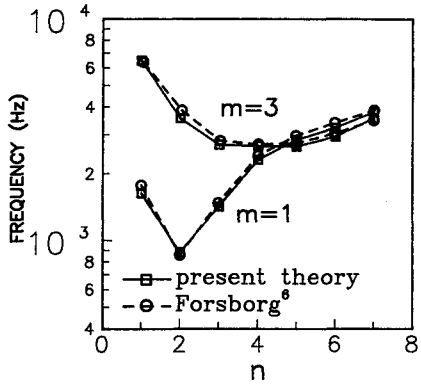

Fig. 4a Natural frequencies of three-ring-stiffened shell with $\Omega = 0$.

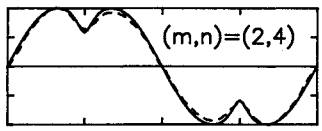

Fig. 4b Mode shapes: $(m,n) = (2,4)$.

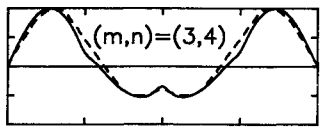

Fig. 4c Mode shapes: $(m,n) = (3,4)$.

As to the case of two rings (attached at ξ_1 and ξ_2), the frequency equation becomes

$$(\alpha_{11} + \beta_1)(\alpha_{22} + \beta_2) - \alpha_{12} \cdot \alpha_{21} = 0 \tag{31a}$$

where α_{12} and α_{21} are the cross receptances of the shell. From Eq. (15), one obtains that

$$\alpha_{12} = \alpha_{21} = -\frac{2}{\rho_s h_s l} \sum_{m=1}^{\infty} \frac{(\hat{a}\hat{d} - \hat{b}^2)}{\Delta_{mn}} \frac{1}{(\omega - \omega_{mn1})(\omega - \omega_{mn2})}$$

$$\times \sin(m\pi\xi_1) \sin(m\pi\xi_2) \tag{31b}$$

where $n = 1, 2, 3, \ldots$.

Numerical Results

The results, specialized for no spinning, are first compared with the data available in the paper of Forsberg.[6] This is a partial verification of the developed approach. Figure 4a shows the natural frequencies for $m = 1$ and 3 with various n for the three-ring shell. The mode shapes for $n = 4$ and $m = 2$ and 3 are also compared in Figs. 4b and 4c. The results, as seen, showed satisfactory agreement. Wilken and Soedel[9] once considered the tangential constraint between ring and shell but with different shell theory. They obtained results close to ours. Hence, it is justified that with the present theory, for lower modes, radial constraints are enough.

The material properties and geometric parameters of the shell and the ring stiffeners demonstrated in this paper are listed in Table 1. Note that the shell and the ring are selected to be the same material in the paper. However, it is not necessary. Parametric studies of the influences of ring properties had been conducted by many researchers as listed in the references. In this paper, emphasis is placed on the spinning effects. One of the methods to the solution of Eq. (27) is the graphic method, in which the left side of Eq. (27) is plotted with varying ω, and the intersections of the curves with abscissa are exactly the solutions. The advantage of the graphic method is that the shifts of shell frequencies due to the stiffening rings are directly seen. Graphic results for the one-ring ($\xi_1 = 0.5$) shell are illustrated in Fig. 5 for $\Omega^* = 0$ and in Fig. 6

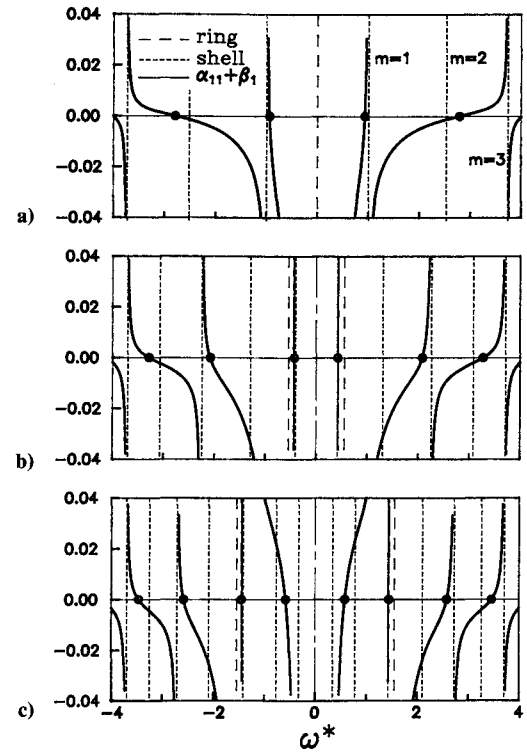

Fig. 5 Graphic method for one-ring-stiffened shell with $\Omega^* = 0$: a) $n = 1$; b) $n = 2$; c) $n = 3$.

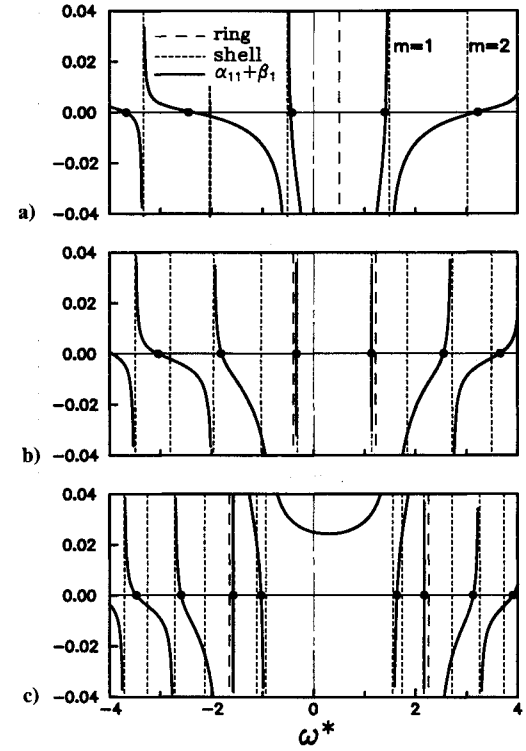

Fig. 6 Graphic method for one-ring-stiffened shell with $\Omega^* = 0.5$: a) $n = 1$; b) $n = 2$; c) $n = 3$.

for $\Omega^* = 0.5$, where $()^* = ()/\omega_{11}$ is a dimensionless parameter and ω_{11} is the $(m,n) = (1,1)$ natural frequency of the stationary shell. Each figure shows three plots for 1) n = a, 2) n = b, and 3) n = c. In these figures, dashed lines denote the natural frequencies of the shell and the ring. The intersections of the curves with the abscissa are exactly the natural frequencies of the ring-stiffened shell. Hence, the effects of frequency

Table 1 Specifications of the demonstrated ring-stiffened shell

Material properties of shell and ring	
Shell	
Density	$\rho = 2.71 \times 10^{-9}$ Ns^2/mm^4
Young's modulus	$E = 7.1 \times 10^4$ N/mm^2
Poisson's ratio	$\nu = 0.33$
Ring	
Density	$\rho = 2.71 \times 10^{-9}$ Ns^2/mm^4
Young's modulus	$E = 7.1 \times 10^4$ N/mm^2
Poisson's ratio	$\nu = 0.33$
Geometric parameters of shell and ring	
Shell	
Mean radius	$a = 77.3$ mm
Length	$l = 411.0$ mm
Radial thickness	$h = 1.52$ mm
Ring	
Mean radius	$a = 77.3$ mm
Width	$b = 5.08$ mm
Radial thickness	$h = 9.14$ mm

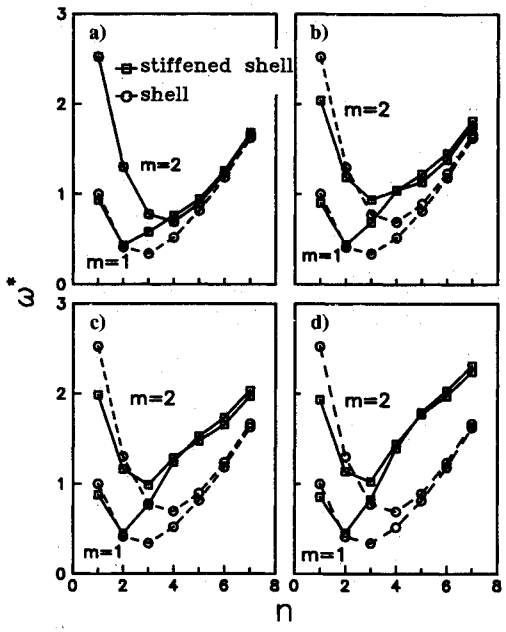

Fig. 7 Natural frequencies of shell and stiffened shell with $\Omega^* = 0$: a) one ring; b) two rings; c) three rings; d) four rings.

changes due to ring stiffeners are clearly observed. In Fig. 5 ($\Omega^* = 0$), it should be noticed that the intersections are symmetrical with the ordinate of $\omega^* = 0$. It is consistent with other investigations on stationary shells, for which the natural frequencies appear in pairs of $+\omega$ and $-\omega$ (Ref. 17). As the rotation enters, e.g., $\Omega^* = 0.5$, as shown in Fig. 6, the intersections are somewhat shifted and the original positive and negative frequencies are then of different values. This phenomenon has been described as the bifurcation of natural frequencies.[15]

Equation (27) is also solved numerically for up to four rings. In the following, the effects of ring stiffeners on frequency changes without and with spinning are illustrated in Figs. 7 and 8, respectively. Figure 9 shows the effects of spinning speed for a four-ring stiffened shell. In Fig. 7, it is noticed that, for lower n, the frequencies of the stiffened shell are always lower than those of the unstiffened shell. For higher n ($n \geq 3$), the frequencies are indeed increased by the presence of rings. This phenomenon is, however, not surprising at all. The ring stiffeners impose, in general, a stiffening effect and a mass loading effect. For the case of $n = 1$, the circular cross section of the shell and rings remain, and the rings impose no stiffening effect. Conversely, the mass effect brings the frequencies to lower values. For higher values of n, as seen in Fig. 7, the stiffening effect becomes dominant and the frequencies are increased by the rings attachment. In Fig. 8, where $\Omega^* = 0.5$, the frequencies of $m = 1$ modes split into two branches due to rotation. The stiffened nonspinning shell frequencies are superimposed as dotted curves to emphasize the bifurcation effect. It needs to be noted that one branch (the lower) is, in fact, comprised of negative frequencies, based on Eq. (14). The figure shows only the absolute values.

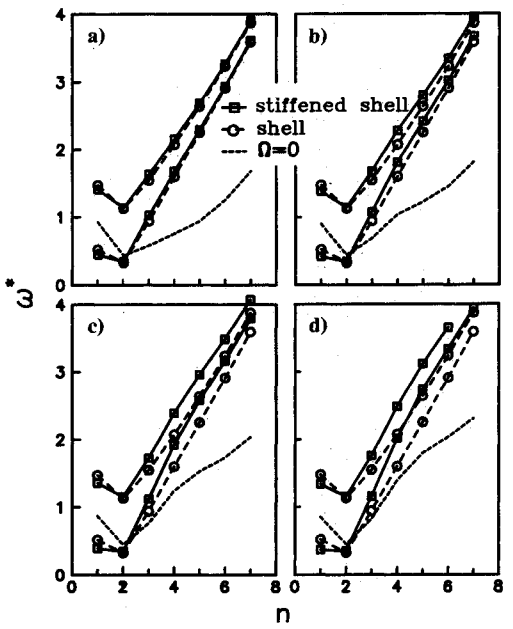

Fig. 8 Natural frequencies of shell and stiffened shell with $\Omega^* = 0.5$: a) one ring; b) two rings; c) three rings; d) four rings.

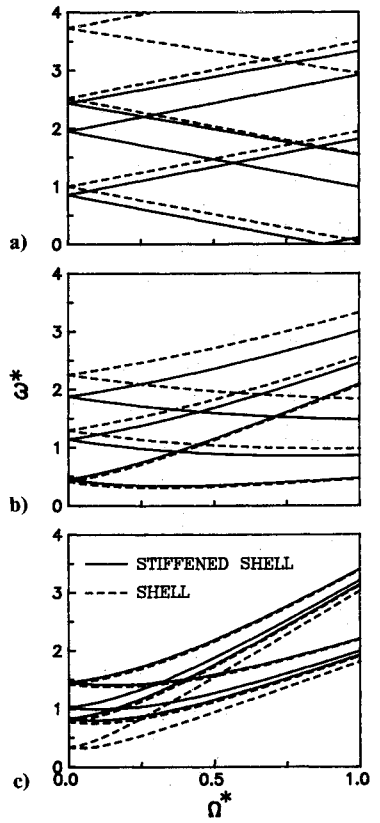

Fig. 9 Natural frequencies of $m = 1$, 2, 3 modes of the spinning four-ring-stiffened shell: a) $n = 1$; b) $n = 2$; c) $n = 3$.

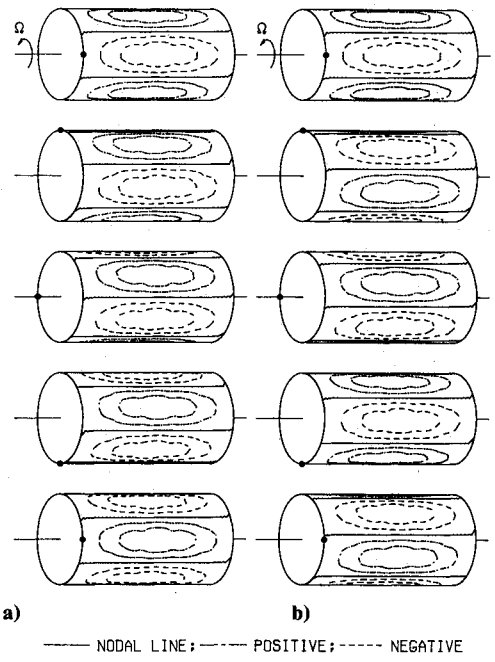

Fig. 10 Forward and backward modes, $(m,n) = (1,3)$, $\Omega^* = 0.5$, shown at five shell orientations: a) backward mode; b) forward mode.

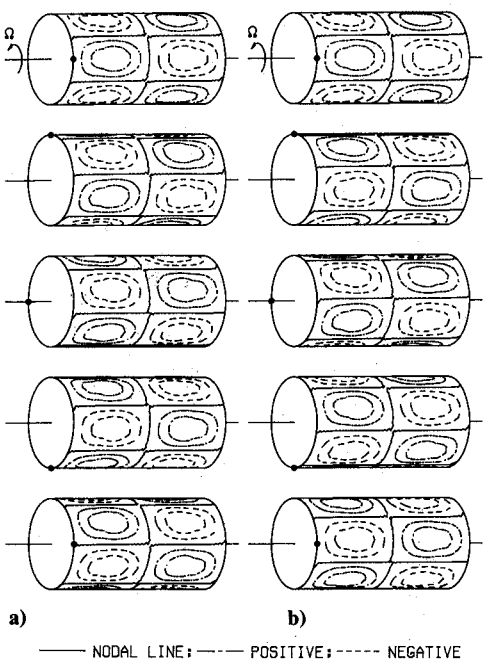

Fig. 11 Forward and backward modes, $(m,n) = (2,3)$, $\Omega^* = 0.5$, shown at five shell orientations: a) backward mode; b) forward mode.

It will be further demonstrated that one of these two branches corresponds to the forward modes and the other to the backward modes. This figure also reveals an important feature: If the spinning shell frequencies were evaluated from the nonspinning shell, tremendous errors could result. Figure 9 shows the spinning speed effects for $n = 1$, 2, and 3 modes. In this figure, the lowest three sets ($m = 1$, 2, 3) of frequencies are illustrated. The natural frequencies of the unstiffened shell are superimposed as dashed curves for comparison. Figure 9 shows that, in addition to frequencies bifurcation, the increase of spinning speed increases the shell frequencies (centrifugal effects) as expected.

To sketch the mode shapes of the spinning reinforced shell, the concept of forced response is applied.[18] The modal forces at attaching lines are solved for from the following equation:

$$\begin{bmatrix} \alpha_{11}(\omega_k)+\beta_1(\omega_k) & \alpha_{12}(\omega_k) & \cdots & \alpha_{1j}(\omega_k) \\ \alpha_{21}(\omega_k) & \alpha_{22}(\omega_k)+\beta_2(\omega_k) & \cdots & \alpha_{2j}(\omega_k) \\ \vdots & \vdots & & \vdots \\ \alpha_{j1}(\omega_k) & \alpha_{j2}(\omega_k) & \cdots & \alpha_{jj}(\omega_k)+\beta_j(\omega_k) \end{bmatrix} \begin{bmatrix} F_1 \\ F_2 \\ \vdots \\ F_j \end{bmatrix} = 0 \tag{32}$$

Where F_i is the modal force magnitude at the ith attachment, and ω_k is the kth frequency. The matrix of Eq. (32) is singular and only the ratios of modal forces are obtained. Applying them as external forces to the spinning shell, the deflective response exactly shows the kth mode shape of the stiffened shell. Some mode shapes for the spinning four-ring stiffened shell are shown in Fig. 10 for $m = 1$ and in Fig. 11 for $m = 2$ at a speed $\Omega^* = 0.5$ These figures show the nodal variances at five shell orientations in one revolution. Corresponding to each (m,n) number, there are two modes. Each mode rotates at its own speed $\Omega - \omega_{mn}/n$ (Ref. 15).

Conclusions

A technique utilizing the receptance method for the vibration analysis of spinning shell-ring structures was developed for the first time. When rotation effects were omitted, the frequency equation of the spinning ring-stiffened shell yielded exactly the same expression as that for stationary shell developed in other references. It was a partial check of the validity of the approach. Numerical results were shown, and the authors have arrived at the following conclusions:

1) The developed approach provided an effective way to evaluate the vibration characteristics of spinning shell-ring structures that were different from stationary ones.

2) The ring stiffeners imposed not only the stiffening effect but also the mass loading effect. For lower mode number n, the mass effect dominated, hence resulting in a decrease of frequencies. When the mode number n was greater than 2, the stiffening effect became important.

3) The frequencies and modes of the spinning structures bifurcated due to Coriolis accelerations.

4) The illustrated results were normalized, hence they showed the unitary trend of these types of structures.

Appendix: Parameters of the Spinning Shell and Ring

The parameters $\hat{a} \sim \hat{f}$ of the shell:

$$\hat{a} = \frac{1}{\rho h}\left[K\left(\frac{m\pi}{l}\right)^2 + K\frac{(1-\nu)}{2}\left(\frac{n}{a}\right)^2 + n^2(\rho h\Omega^2)\right] \tag{A1}$$

$$\hat{b} = \frac{1}{\rho h}\left[\frac{(1+\nu)nK}{2a}\left(\frac{m\pi}{l}\right)\right] \tag{A2}$$

$$\hat{c} = \frac{1}{\rho h}\left[\frac{\nu K}{a}\left(\frac{m\pi}{l}\right)\right] \tag{A3}$$

$$\hat{d} = \frac{1}{\rho h}\left[n^2\left(\frac{D}{a^4}+\frac{K}{a^2}+\rho h\Omega^2\right) + \frac{(1-\nu)}{2}\left(K+\frac{D}{a^2}\right)\left(\frac{m\pi}{l}\right)^2\right] \tag{A4}$$

$$\hat{e} = \frac{n}{\rho h}\left[n^2\frac{D}{a^4} + \frac{K}{a^2} + 2\rho h\Omega^2 + \frac{D}{a^2}\left(\frac{m\pi}{l}\right)^2\right] \tag{A5}$$

$$\hat{f} = \frac{1}{\rho h}\left[n^4\frac{D}{a^4} + \frac{K}{a^2} + n^2(\rho h\Omega^2) + \frac{2n^2D}{a^2}\left(\frac{m\pi}{l}\right)^2 + D\left(\frac{m\pi}{l}\right)^4\right] \tag{A6}$$

The parameters $\bar{a} \sim \bar{c}$ of the ring:

$$\bar{a} = \frac{1}{\rho h}\left(n^3\frac{D}{a^4} + n\frac{K}{a^2}\right) + 2n\Omega^2 \tag{A7}$$

$$\bar{b} = \frac{1}{\rho h}n^2\left(\frac{D}{a^4} + \frac{K}{a^2}\right) + n^2\Omega^2 \tag{A8}$$

$$\bar{c} = \frac{1}{\rho h}\left(n^4\frac{D}{a^4} + \frac{K}{a^2}\right) + n^2\Omega^2 \tag{A9}$$

Acknowledgment

The authors are grateful to the National Science Council of the Republic of China for the support under Grant 79-0401-E011-06.

References

[1]Huang, S. C., and Soedel, W., "Effects of Coriolis Acceleration on the Forced Vibration of Rotating Cylindrical Shells," *Journal of Applied Mechanics,* Vol. 55, No. 1, 1988, pp. 231–233.

[2]Huang, S. C., and Soedel, W., "Effects of Coriolis Acceleration on the Free and Forced In-plane Vibrations of Rotating Rings on Elastic Foundation," *Journal of Sound and Vibration,* Vol. 115, No. 1, 1987, pp. 253–274.

[3]Wah, T., and Hu, W. C. L., "Vibration Analysis of Stiffened Cylinders Including Inter-Ring Motion,"*Journal of the Acoustical Society of America,* Vol. 43, No. 5, 1968, pp. 1005–1016.

[4]Garnet, H., and Levy, A., "Free Vibrations of Reinforced Elastic Shells," *Journal of Applied Mechanics,* Vol. 36, No. 4, 1969, pp. 835–844.

[5]Al-Najafi, A. M. J., and Warburton, G. B., "Free Vibration of Ring-Stiffened Cylindrical Shells," *Journal of Sound and Vibration,* Vol. 13, No. 1, 1970, pp. 9–25.

[6]Forsberg, K., "Exact Solution for Natural Frequencies of a Ring-Stiffened Cylinder," AIAA/ASME 10th Structures, Structural Dynamics and Materials Conference, ASME Volume on Structures and Materials, 1969, pp. 18–30.

[7]Beskos, D. E., and Oates, J. B., "Dynamic Analysis of Ring-Stiffened Circular Cylindrical Shells," *Journal of Sound and Vibration,* Vol. 75, No. 1, 1981, pp. 1–15.

[8]Bishop, R. E. D., and Johnson, D. C., *The Mechanics of Vibration,* Cambridge Univ. Press, 1960, Chap. 1.

[9]Wilken, I. D., and Soedel, W., "The Receptance Method Applied to Ring-Stiffened Cylindrical Shells: Analysis and Modal Characteristics," *Journal of Sound and Vibration,* Vol. 44, No. 4, 1976, pp. 563–576.

[10]Wilken, I. D., and Soedel, W., "Simplified Prediction of the Modal Characteristics of Ring-Stiffened Cylindrical Shells," *Journal of Sound and Vibration,* Vol. 44, No. 4, 1976, pp. 577–589.

[11]Kelkel, K., "Green's Function and Receptance for Structures Consisting of Beams and Plates," *AIAA Journal,* Vol. 25, No. 11, 1987, pp. 1482–1489.

[12]Huang, S. C., and Hsu, B. S., "Resonant Phenomena of a Rotating Cylindrical Shell Subjected to a Harmonic Moving Load," *Journal of Sound and Vibration,* Vol. 136, No. 2, 1990, pp. 215–228.

[13]Leissa, A. W., "Vibration of Shells," NASA SP-288, 1973, Chap. 2.

[14]Huang, S. C., and Soedel, W., "On the Forced Vibration of Simply Supported Rotating Cylindrical Shells," *Journal of the Acoustical Society of America,* Vol. 84, No. 1, 1988, pp. 275–285.

[15]Huang, S. C., "Effects of Coriolis Acceleration on the Vibration of Spinning Structures," Ph.D. Dissertation, Purdue Univ., Mechanical Engineering Dept., West Lafayette, IN, May 1987.

[16]Huang, S. C., and Soedel, W., "Response of Rotating Rings to Harmonic and Periodic Loading and Comparison with the Inverted Problem," *Journal of Sound and Vibration,* Vol. 118, No. 2, 1987, pp. 253–270.

[17]Soedel, W., *Vibration of Shells and Plates,* Marcel Dekker, New York, 1981, pp. 315–321.

[18]Huang, S. C., and Hsu, B. S., "Theory of Receptance Applied to Modal Analysis of Spinning Disk with Interior Multi-Point Supports," *Journal of Vibration and Acoustics* (to be published).